SCHOLARLY PUBLICATIONS
School of Applied Sciences
KIIT Deemed to be University

Journal Name: Advanced Materials **IF: 26.8**

Title: Quadruple Moiré Pockets in Lateral Heterobilayers: Programmable Phononic Reconfiguration and Anomalous Second Harmonic Generation

Author: Chakraborty, S.K.; Ray, P.; Sousa, F.B.; Sahoo, C.; Prasad, I.D.; Biswas, S.; Nayak, B.; Kundu, B.; Rojas, R.; Jones, A.J.H.; Miwa, J.A.; Ulstrup, S.; Dutta, S.; Kumar, S.; Malard, L.M.; Pradhan, G.K.; Sahoo, P.K.

Details: Volume 38, Issue 8**,** February 2026

Abstract: Moiré-engineering in 2D transition-metal dichalcogenides offers access to correlated quantum phenomena. However, simultaneous control over twist-angle (θ) and material combinations to tune phonons, excitons, and their collective interactions remains limited. This study presents scalable, quadruple moiré-pockets formed by vertically stacking chemical vapor deposition-grown monolayer MoS_2–WS_2 and $MoSe_2$–WSe_2 lateral heterostructures with controlled θ (0^o–60°), within a single flatland. Moiré non-rigidity induces lattice-relaxation via rotational reconstruction (θ<8°) and volumetric dilation (θ>8°), resulting in strain-mediated phonon frequency-softening and linewidth-broadening, respectively. Strain localizes selectively in mechanically softer crystal for θ<8°, while an epitaxial-pseudomorphic pattern dominates for θ>8°. Degree of phonon-reconfiguration and angle-resolved photoemission spectroscopy uncover the role of interfacial orbitals in modulating interlayer coupling. At aligned angles (θ–0° and 60°), specifically, MoS_2 exhibits Davydov splitting and reduced valley polarization, reflecting symmetry breaking and chiral phonon effects. At θ–3°, WS_2/WSe_2 shows up to 480% enhancement in second-harmonic generation (SHG), while $WS_2/MoSe_2$ records the lowest due to variations in interlayer-coherence and band-offset-driven phase delay. Notably, at θ–60°, only $WS_2/MoSe_2$ exhibits an anomalous 300% SHG enhancement, attributed to large phase delay and reconstruction-induced strain. Electronic bandstructure calculations support these observations. These findings offer programmable multi-moiré platforms for opto-straintronics, sensing, and on-chip quantum photonics applications.

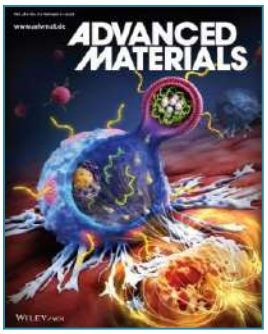

URL: https://advanced.onlinelibrary.wiley.com/doi/10.1002/adma.202520008

SCHOLARLY PUBLICATIONS
School of Applied Sciences
KIIT Deemed to be University

Journal Name: Acs Applied Materials & Interfaces **IF: 8.2**

Title: The Crucial Role of Hydrogen Ligation in the Stability of Single Atoms on Rutile TiO2: A First-Principles Study

Author: Ghoshal, S; Ezeakunne, C; Lee, Y; Alexandrova, AN; Kattel, S

Details: Volume 18 , volume 7, February 2026

Abstract:. Understanding the stability of TiO2-supported single-atom catalysts (SACs) under H-2 reduction conditions, where hydrogen adsorption on the metal/TiO2 surface influences metal-support interactions, diffusion, and aggregation, is important for their long-term applications. Using first-principles density functional theory (DFT) calculations, we investigate the thermodynamic and kinetic stability of Rh, Ag, Pt, and Au-based SACs on pristine, oxygen-defective, and hydroxylated rutile TiO2 (110) surfaces with and without H adsorption on the metal adatom. The thermodynamic driving force for aggregation was assessed by calculating dimerization energies as proxy, while the kinetic stability was quantified in two ways: (i) the total activation energy, E-total (E-f + E-d), which couples adatom formation (E-f) and diffusion (E-d) energies, serves as a descriptor of ripening kinetics, and (ii) the E-d, used to evaluate diffusion rate constants and characteristic diffusion times, tau. The results show that Pt consistently exhibits the largest E-total and longest tau, reflecting exceptional resistance to sintering, whereas Ag has the smallest values and is intrinsically unstable. Rh presents a distinctive case: although dimerization is thermodynamically favored, its E-total is dominated by the formation energy of two separated Rh atoms on support (*Rh*Rh), giving Rh longer lifetimes than expected from its low diffusion barrier for dimer (*Rh-2) formation. Au is unstable on oxygen-deficient TiO2 but is kinetically stabilized upon hydroxylation, which significantly increases both E-total and tau. Hydrogen adsorption further modulates stability in a metal-dependent manner-stabilizing Rh but accelerating the aggregation of Ag and Au. This combined thermodynamic-kinetic framework provides a quantitative basis for predicting SAC sintering behavior and guiding strategies for stabilizing late transition metals under hydrogenation conditions.

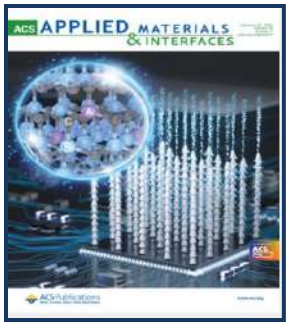

URL: https://pubs.acs.org/doi/10.1021/acsami.5c24310

Journal Name: Measurement: Journal of the International Measurement Confederation **IF: 5.6**

Title: An IoT based novel data logger and controller and normalized gain calculator for gaseous detector

Author: Panigrahi, S.S.; Nayak, A.; Sahu, S.K.; Sahu, P.K.

Details: Volume 268, April 2026

Abstract: Maintaining a clean and controlled environment in the Detector Laboratory is critical for optimal performance of gaseous and solid-state detectors. An IoT based environmental data logger and controller has a wide functional advantage over the traditional data loggers. The system described in this paper allows for real-time monitoring of these parameters as well as tracking particle concentrations, including mass and number concentrations for various particles sizes. The local controls and data logging of different parameters are based on the LabVIEW interface. The data acquisition circuits enable data collection for experiments such as gaseo us detectors as well as solid-state detectors. This advancement provides a robust comprehensive and remotely accessible solution for laboratory environmental monitoring. The developed DAQ system is not only suitable for environmental monitoring but also for determining the temperature (T) and pressure (p) - dependent gain (G) of GEM detectors. For demonstration purpose, a quad-GEM detector has been used to perform an experiment and T/p and the corresponding G(T/p) is calculated in real-time using the proposed DAQ system, in an attempt to implement the T/p compensation in the detector gain. At an ambient temperature of T=294.462K and a pressure of p=1010.150mbar (0.996atm), the corresponding T/p ratio is 295.644K/atm. Under these conditions, the quad-GEM detector exhibited a gain of (4.326±0.067) $\times 10^4$, as estimated by the DAQ software, with a particulate matter concentration of PM2.5=3.6µg/cm^3.

URL: https://www.sciencedirect.com/science/article/pii/S0263224126004021?via%3Dihub

SCHOLARLY PUBLICATIONS
School of Applied Sciences
KIIT Deemed to be University

Journal Name: Inorganic Chemistry Communications **IF: 5.4**

Title: Nanozyme-based remediation of complex wastewater streams: a focus on emerging contaminants

Author: Nayak, S.; Hansdah, S.; Palai, S.P.; Malik, G.C.; Singh, B.; Fawcett, D.; Poinern, G.E.J.; Parhi, P.K.

Details: Volume 186, April 2026

Abstract: The increasing prevalence of water pollution, driven by contaminants such as heavy metals, dyes, pharmaceuticals, and microplastics, necessitates innovative approaches to wastewater treatment. Nanozymes-synthetic nanomaterials with enzyme-like catalytic properties - have emerged as a promising alternative to conventional enzymes due to their superior stability, tunable activity, and cost-effective production. This review provides a comprehensive analysis of nanozyme synthesis methods, including chemical, biological, green, and physical approaches, alongside their catalytic mechanisms such as reactive oxygen species (ROS) generation and redox reactions. Applications of nanozymes in degrading organic pollutants, heavy metals, and emerging contaminants like microplastics are critically examined. This includes degradation of persistent and emerging contaminants such as pharmaceuticals and microplastics, which pose significant challenges to conventional treatment methods. Special attention is given to metal-organic frameworks (MOFs) as synergistic supports that enhance nanozyme performance through improved stability and pollutant specificity. While many challenges remain, regarding long-term environmental impacts and large-scale implementation, this review underscores the transformative potential of nanozymes in addressing global water pollution. By bridging the gap between fundamental research and practical applications, this study aims to inspire future innovations in sustainable water management.

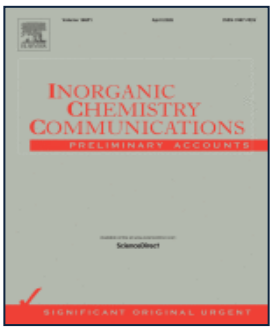

URL: https://www.scopus.com/pages/publications/105029116655?origin=resultslist

SCHOLARLY PUBLICATIONS
School of Applied Sciences
KIIT Deemed to be University

Journal Name: Diamond And Related Materials **IF: 5.1**

Title: Selective, Non-Enzymatic Electrochemical Detection of Dopamine Using a Green-Synthesized CuO/rGO Nanocomposite-Modified Electrode

Author: Deo, R; Devi, M

Details: Volume 163 , March 2026

Abstract:. A non-enzymatic electrochemical sensor was developed for selective detection of dopamine (DA) in the presence of ascorbic acid (AA) using copper oxide (CuO) and green-synthesized reduced graphene oxide (rGO) nanocomposite modified graphite electrode (GE). An easy, cost-effective ultrasonication method was adopted for the synthesis of the nanocomposite. The structural, morphological, elemental and optical characterization was done by X-ray diffraction (XRD), Raman, Field emission scanning electron microscopy (FESEM), Energy dispersive spectroscopy (EDS), Ultraviolet Visible spectroscopy (UV–Vis) and Fourier-transform infrared spectroscopy (FTIR). Electrochemical studies using the modified electrode for the detection of DA were performed using cyclic voltammetry (CV), electrochemical impedance spectroscopy (EIS) and differential pulse voltammetry (DPV) techniques. CV study reveals the enhanced redox mechanism towards DA due to the synergetic effect of the catalytic CuO and highly conductive rGO nanocomposite, which was further confirmed by greater electron transfer rate, studied from EIS. From the DPV plot, the limit of detection was calculated to be 1.84 µM with the wide linear range of 1–300 µM for DA. The selective detection of DA was carried out in the presence of AA. The modified electrode shows satisfactory results for reproducibility, repeatability and long-term stability. The detection of DA in human blood serum confirmed the recovery up to 104%, which shows its efficacy for real-world utilization.

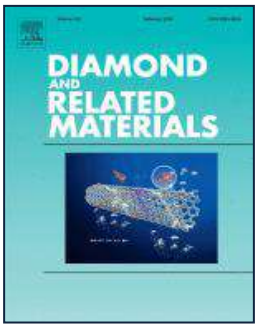

URL: https://www.sciencedirect.com/science/article/pii/S0925963526001184?via%3Dihub

SCHOLARLY PUBLICATIONS
School of Applied Sciences
KIIT Deemed to be University

Journal Name: Polymers **IF: 4.9**

Title: Development of UV-Resistant Chitosan/Starch Biofilms Reinforced with Chitosan Nanoparticles for Sustainable Packaging

Author: Yadav M.; Maurya P.; Dash P.; Seth A.; Yadav D.; Jain M.; Tripathy J.; Sand A.; Chandra P.; Panda P.K.

Details: Volume 18, Issue 5, March 2026

Abstract: The fabrication of sustainable packaging films based on chitosan/starch (CTS/Starch) blends, reinforced with Chitosan Nanoparticles (CNPs), was achieved via the casting blend technique. This research explored the impact of varying CNPs loading on critical physicochemical properties, including water vapor permeation (WVP), thermal stability, and mechanical strength. The reduction in WVP from 6.18 ± 0.54 to 5.38 ± 0.93 $g.m^{-1}.s^{-1}.pa^{-1}$, equilibrium moisture content (EMC) from 16.52 ± 1.03% to 12.5 ± 1.05%, and water absorbency (WA) from 340 ± 1.63% to 88.65 ± 1.12% in CTS/Starch blend films demonstrated loaded with (0–8 wt%) CNPs loading. Concurrently, films with 2–8 wt% CNP loading exhibited an increase in opacity from 2.38 ± 1.01 mm^{-1} to 4.83 ± 0.83 mm^{-1}, accompanied by a decrease in transmittance from 89.20 ± 0.50% to 79.70 ± 1.20%. These findings collectively indicated that the CNP-incorporated chitosan/starch composites offer enhanced ultraviolet light shielding and improved water barrier capabilities compared to the non-reinforced chitosan/starch films, underscoring their promising utility in food and pharmaceutical packaging applications.

URL: https://www.mdpi.com/2073-4360/18/5/662

SCHOLARLY PUBLICATIONS
School of Applied Sciences
KIIT Deemed to be University

Journal Name: Journal of Physics and Chemistry of Solids **IF: 4.9**

Title: Unlocking the potential of NiO@BiFeO3 nanocomposite for high-performance supercapacitor electrodes

Author: Rout, S.K.; Samal, P.K.; Panigrahy, J.; Nanda, P.; Pati, B.; Praharaj, S.; Rout, D.

Details: Volume 210, March, 2026

Abstract: The pursuit of electrochemical supercapacitors offering superior energy and power densities has necessitated intensive research into efficient electrode materials. This study explores the potential of NiO@$BiFeO_3$ nanocomposite series as an electrode material. X-ray diffraction confirms the formation of nanocomposites with $Bi_2Fe_4O_9$ as a minor phase, and Rietveld refinement determines their phase percentages. In a three-electrode setup, BN50 (50 wt% $BiFeO_3$ + 50 wt% NiO) demonstrates an excellent specific capacitance of 772 F g^{-1} (at 1 mV/s) and a discharge time of 1080 s (at 0.5 A g^{-1}) from −0.3 to +0.8 V. It is related to the abundance of oxygen vacancies and the existence of multiple oxidation states (XPS), well-interconnected network of irregular particles with minimal agglomerations (FESEM) and synergistic effect of the components in BN50 compared to $BiFeO_3$. A remarkable capacity retention of 120 % is sustained over 20,000 cycles in BN50. Moreover, BN50//BN50 symmetric device exhibits a specific capacitance of 141.68 F g^{-1} at 5 mV/s and delivers an energy density of 28 W h/kg at a power density of 375 W/kg. Two such symmetric cells (series) could power a red LED (1.8 V) up to 10 min. Overall, this work highlights the suitability of NiO@$BiFeO_3$ as a highly redox-active electrode material for charge storage.

URL: https://www.sciencedirect.com/science/article/pii/S0022369725007838?via%3Dihub

SCHOLARLY PUBLICATIONS
School of Applied Sciences
KIIT Deemed to be University

Journal Name: Journal of Physics and Chemistry of Solids **IF: 4.9**

Title: An ab-initio investigation of Cd-based defect chalcopyrite-type semiconductors: Promising candidates for sustainable energy goals

Author: Nayak, A.; Jena, S.; Parida, P.

Details: Volume 212 May 2026

Abstract: This work focuses on the thermoelectric behavior of CdGaX (X = S, Se, and Te) defect chalcopyrite compounds, carried out using density functional theory (DFT) within the generalized gradient approximation (GGA). The ab-initio structural analysis of these body-centered tetragonal compounds reveals a systematic increase in lattice parameters from CdGaS to CdGaTe, along with the deviation from the ideal chalcopyrite structure. CdGaS exhibits the highest thermodynamic stability, having the lowest cohesive energy. The value of lowest defect formation energy of all the compounds confirmed that the formation of the defects can be done easily. The electronic properties show that all three systems are direct band gap semiconductors. The ductile nature of these compounds is obtained from the elastic behaviors, with CdGaS having the maximum stiffness. All the compounds are found to be thermally stable at elevated temperature (at 800K) through AIMD calculations. The electronic thermoelectric properties are calculated using the semi-classical Boltzmann transport theory. The thermoelectric parameters are calculated w.r.t. temperature, carrier concentration, and chemical potential, revealing enhanced performance under p-type doping. CdGaS and CdGaSe show peak ZT values at high temperatures with a carrier concentration of 10^{18} cm^{-3}, while CdGaTe peaks at 10^{20} cm^{-3}. Using the deformation potential theory and Slack method, the carrier relaxation time and the lattice thermal conductivity are determined, respectively. This study highlights the potential of CdGaX compounds as promising thermoelectric materials, especially at elevated temperatures.

URL: https://www.sciencedirect.com/science/article/pii/S0022369726000235?

SCHOLARLY PUBLICATIONS
School of Applied Sciences
KIIT Deemed to be University

Journal Name: Journal of Physics and Chemistry of Solids **IF: 4.9**

Title: Structural, microstructural, impedance spectroscopy and dielectric studies on La2Co1-xZnxMnO6 (x=0, 0.05 and 0.1) double perovskite

Author: Mohanty, S.; Biswal, A.K.; Ray, J.

Details: Volume 211, April 2026

Abstract: $La_2Co_{1-x}Zn_xMnO_6$ (x = 0, 0.05 and 0.1) samples were synthesized via the sol–gel auto-combustion method and systematically characterized. Rietveld refinement of room-temperature X-ray diffraction confirmed a single-phase monoclinic structure (space group $P2_1/n$), with negligible change in lattice parameters at 5 % Zn substitution but a pronounced expansion at 10 %. Analysis of FESEM images revealed the increase in average grain sizes: 112 ± 35 nm (x = 0), 121 ± 36 nm (x = 0.05) and 187 ± 66 nm (x = 0.1), with reduced porosity:15.3 % (x = 0), 14 % (x = 0.05) and 5.74 % (x = 0.1) upon Zn doping. Impedance spectra analysed using the Havriliak–Negami model yielded resistance (R), relaxation time (), asymmetry (α), and broadness (β) parameters, showing a significant rise in R and for the 10 % doped sample across all temperatures. A.C. electrical transport examined from temperature dependent 'R' followed variable-range hopping (VRH), with Mott temperatures () of 1.186×10^9 K, 1.54×10^9 K, and 6.568×10^9 K for x = 0, 0.05, and 0.1, respectively. Density of states of the charge carriers at the Fermi level are $ev^{-1}.cm^{-3}$ for x = 0, $ev^{-1}.cm^{-3}$ for x = 0.05 and $ev^{-1}.cm^{-3}$ for x = 0.1.. The respective activation energies are 0.37 eV, 0.44 eV, 0.79 eV and 0.034 eV for x = 0, 0.05, 0.1 and shallow trap state of x = 0.1 respectively. DC conduction also followed VRH with values K, K and K for x = 0, 0.05 and 0.1 respectively. Also, the temperature window for intrinsic and D increased with Zn substitution. Cole–Cole analysis further revealed well-resolved semi-circles corresponding to the low frequency Maxwell-Wagner contribution and high frequency shallow trap state exclusively for the 10 % doped sample.

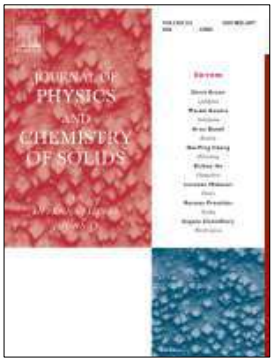

URL: https://www.sciencedirect.com/science/article/pii/S0022369725009503?

SCHOLARLY PUBLICATIONS
School of Applied Sciences
KIIT Deemed to be University

Journal Name: Acs Applied Bio Materials **IF: 4.7**

Title: Divergence in Cu(II)- and Zn(II)-Based Coordination Polymers: The Sensing of Melatonin and Tryptophan, and Their Anticancer Activity

Author: Saha, K; Bhar, S; Jana, NC; Sepay, N; Dutta, B; Jana, SR; Chandra, A; Sinha, C

Details: Volume 9 , Issue 5, February 2026

Abstract: Accurate and selective recognition of ions and molecules is crucial in medical and diagnostic research. Cu(II)- and Zn(II)-based coordination polymers (CPs) have been designed in this work to detect trace levels of melatonin and tryptophan and evaluate their anticancer activity. The [Cu2(4-bph)2(adc)4] n (CP1) (4-bph = (1E,2E)-1,2-bis(pyridin-4-ylmethylene) hydrazine; Hadc = 1-adamantanecarboxylic acid) structure shows that 4-bph serves as a bridging pyridyl-N ligand and adc- is a chelating and binuclear bridging ligand, forming an eight-membered Cu(mu-COO)2Cu motif. In Zn(II)-CP, 4-bph is a bridging ligand, while adc- is monodentate, yielding [Zn(4-bph)(adc)2] n (CP2). In CP1, pi-pi stacking (similar to 3.875 & Aring;) and hydrogen bonding generate a 3D supramolecular network while CP2 forms pyridyl-N bridging zigzag 1D CP. The BET analysis measures higher pore volume of CP1 (0.06 cm3 g-1) than CP2 (0.018 cm3 g-1). The CP1 is weakly emissive, and upon irradiation at 312 nm, it emits at 392 nm which has been enhanced by the addition of tryptophan (Trp) (LOD, 44.65 nM), in the presence of 19 other amino acids. The CP1 senses melatonin (MEL) (LOD, 38 nM) also in the presence of various proteins, enzymes, and neuroactive metal ions. Blood serum is used for the measurement of melatonin in blood serum (pH 7.4) and also tryptophan measurement in milk. The CP2 is inactive toward sensing performance. DFT computation using crystallographic parameters reveals a stronger binding of CP1 with Trp (-221 kcal mol-1) than that of CP2 (-38.22 kcal mol-1). Anticancer assays show that CP1 is more potent than CP2 against MCF-7 breast cancer cells, IC50 values are 196.8 +/- 2.31 nM (CP1) and 258.2 +/- 2.08 nM (CP2). Both CPs exhibit minimal toxicity toward normal PBMCs at these doses. Theoretical evaluation has also been used to explain the luminescence and selective sensing behavior to Trp and MEL.

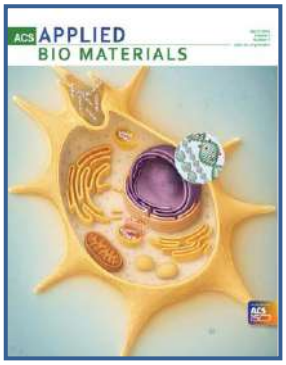

URL: https://pubs.acs.org/doi/10.1021/acsabm.5c02107

SCHOLARLY PUBLICATIONS
School of Applied Sciences
KIIT Deemed to be University

Journal Name: Materials Science and Engineering: B **IF: 4.6**

Title: Insight into the structural and electrical properties of acceptor-doped Na0.5Bi0.5TiO3 system synthesized by microwave-assisted solid-state reaction route

Author: Teki, K.; Mohanty, H.S.; Bhoi, K.; Karmakar, S.; Borkar, H.; Das, D.; Mohapatra, S.

Details: Volume 325 **,** March 2026

Abstract: In this report, microwave-assisted solid-state synthesis route was employed to fabricate B-site acceptor-doped NBT ferroelectric ceramic oxide $(Na_{0.5}Bi_{0.5})Ti_{(1-x)}Mg_xO_3$, $(0.00 \leq x \leq 0.08)$. The effect of varying magnesium doping levels on the phase formation, microstructure, dielectric behavior, and ferroelectric response was analyzed and discussed. The presence of a single-phase rhombohedral structure (R3c space group) for both the parent and substituted compounds is confirmed by room temperature XRD analysis in conjunction with structural Rietveld refinement and Raman analysis. The unit cell volume increases with Mg substitution. UV–visible spectroscopy analysis indicates a decrease in the band gap from 3.01 eV to 2.68 eV upon Mg substitution. A relatively open, nano-saturated ferroelectric hysteresis loop is observed for pure NBT, whereas the loop becomes slimmer for the Mg-substituted sample, suggesting relaxor behavior. The temperature-dependent dielectric constant of NBT exhibits a distinct anomaly around 200–250 °C, corresponding to the ferroelectric phase transition. This transition shifts towards a lower temperature range (100–200 °C) with Mg substitution. Another dielectric anomaly is observed above 300 °C for NBMT, where the dielectric constant reaches its maximum value. The Nyquist analysis provides valuable insights into the structure-property relationship of the materials. The frequency-dependent AC conductivity data were analyzed using the universal power law to determine the dominant conduction mechanism, while activation energies extracted from temperature-dependent impedance measurements were used to identify the type of charge carriers participating in the electrical processes.

URL: https://www.sciencedirect.com/science/article/pii/S0921510725011353?via%3Dihub

SCHOLARLY PUBLICATIONS
School of Applied Sciences
KIIT Deemed to be University

Journal Name: RSC Advances **IF: 4.6**

Title: Enhanced visible-light-driven photocatalytic degradation of methylene blue and ciprofloxacin using magnetic NiFe2O4@ZIF 67

Author: Priyadarshini A.; Das N.; Soren S.; Panda S.P.; Swain S.; Panda J.; Chandra Dhal B.; Swain J.; Acharya D.; Ghosh S.; Sahu R.

Details: Volume 16, Issue 12, February 2026

Abstract: Designing metal organic framework (MOF)-based stable heterostructures remains a challenging task for material scientists. Herein, a magnetic photocatalyst, designated 30NFZ67, was synthesized using a simple and green method by combining ZIF 67 and $NiFe_2O_4$ at room temperature. The fabrication of a hybrid MOF material was characterized using various techniques, such as IR spectroscopy, PXRD, XPS, TGA, FESEM, and TEM, which revealed the successful formation of a heterostructure. Under sunlight, the photocatalyst effectively degraded two major organic pollutants methylene blue (MB) dye (~98%) and ciprofloxacin (CIP) antibiotic (~88%) via a multistep charge transfer mechanism. This process is primarily driven by solar energy, highlighting its potential for sustainable environmental remediation. Trapping experiments identified hydroxyl radicals ($^{\cdot}OH$) and superoxide radicals ($^{\cdot}O_2^-$) as the dominant reactive species in the degradation pathway. The degradation efficiency significantly increased with catalyst dosage, increasing from 72% to 98% for methylene blue (MB) as the dosage increased from 2.5 mg to 10 mg. In alignment with the United Nations Sustainable Development Goal 6 (clean water and sanitation), this work addresses the urgent challenge of emerging organic pollutants in wastewater. Hence, this work highlights the potential of a sustainable and recyclable photocatalyst for wastewater treatment.

URL: https://pubs.rsc.org/en/content/articlelanding/2026/ra/d5ra09822j

SCHOLARLY PUBLICATIONS
School of Applied Sciences
KIIT Deemed to be University

Journal Name: Radiation Physics and Chemistry **IF: 4.3**

Title: Elemental, morphological and radiation-protective nature of selected low-cost construction materials: Experimental, theoretical and PHITS simulation

Author: Upadhyay D.R.; Khatiwada L.N.; Sunar R.; Praharaj S.; Rout D.; Khanal R.

Details: Volume 244, July 2026

Abstract: The ionizing radiation protective nature at different ranges of energy becomes important in materials. The prime objectives of this work are to investigate density, porosity, elemental, minerological, morphological and radiation shielding properties of low cost construction materials (CM). For this seven varieties of CM are experimentally analyzed using Archimedes principle, energy dispersive X-ray fluorescence, FESEM-EDS, powder X-ray diffraction, theoretical and simulation methods. Comprehensive elemental analysis and mapping demonstrated that Si, Ca, Al, O, and Fe constitute the predominant elemental components of the samples. FESEM analysis revealed well-defined crystalline morphologies and the development of microstructural porosity in selected specimens, while XRD patterns confirmed their crystalline nature. Phase assemblage analysis identified quartz (SiO_2), calcite ($CaCO_3$), alumina (Al_2O_3), and hematite (Fe_2O_3) as the dominant mineralogical constituents. Furthermore, the Particle and Heavy Ion Transport code system (PHITS) was used to determine and evaluate the protective nature, such as attenuation coefficients, radiation protection efficiency, transfer factors, and lead equivalent thickness. Moreover, shielding properties are compared with Phy-X/PSD database. Using Phy-X/PSD, the parameters such as linear, mass attenuation, half and tenth value layers, mean free path, effective conductivities, atomic number, and electron densities were estimated. Furthermore, the neutron shielding is also evaluated using both techniques. indicating significant radiation shielding potential. These findings support their suitability as low-cost, environmentally sustainable materials for radiation shielding applications.

URL: https://www.sciencedirect.com/science/article/abs/pii/S0969806X26002112?via%3Dihub

SCHOLARLY PUBLICATIONS
School of Applied Sciences
KIIT Deemed to be University

Journal Name: Results in Chemistry **IF: 4.2**

Title: Eco-sustainability of periphyton-inhabited polyvinyl chloride (PVC) and fibre-reinforced plastic (FRP) inferred by in vivo zebrafish embryo oxidative and steatosis responses

Author: Sahoo M.; Naser S.S.; Jena S.; Gupta A.; Barik D.; Sinha A.; Ghosh A.; Vinod C.; Verma S.K.

Details: Vol. 23, May 2026

Abstract: The growing use of synthetic materials in aquaculture, such as polyvinyl chloride (PVC) and fibre reinforced plastic (FRP), has prompted concerns regarding their environmental and biological safety. Despite their durability and cost-effectiveness, the ecological impact of these materials, especially when colonized by periphyton, remains underexplored. This study investigates the developmental and physiological responses of zebrafish embryos (Danio rerio) exposed to water containing periphyton-covered PVC and FRP sheets. Survivability, morphological development, hatching success, heart rate, and cellular responses were evaluated to understand potential toxic effects. While periphyton biofilms were expected to promote ecological compatibility, findings revealed that both periphyton-inhabited PVC and FRP adversely affected embryonic development. Notable effects included delayed hatching, elevated mortality, and increased oxidative stress. However, PVC exhibited relatively higher biocompatibility, causing fewer disruptions to embryo viability and cellular function compared to FRP. At the molecular level, FRP induced stronger toxic responses, likely due to its chemical composition and more aggressive interaction with developing embryos. In contrast, PVC's material characteristics and associated biofilm interactions were less harmful. The study highlights the importance of assessing both material type and biofilm dynamics in aquaculture systems and supports the shift toward eco-compatible infrastructure for sustainable aquatic practices.

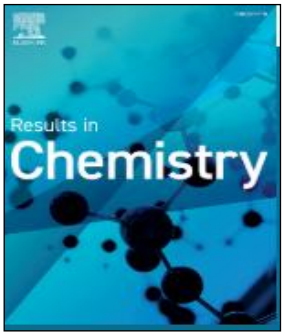

URL: https://www.sciencedirect.com/science/article/pii/S221171562600158X?via%3Dihub

Journal Name: Journal of Solid State Chemistry **IF: 3.5**

Title: Role of transition metal substitution in ZnGa2S4 for intermediate band solar cells: A DFT-driven route toward sustainable energy applications

Author: Jena, S.; Priyambada, A.; Behera, S.S.; Parida, P.

Details: Volume 356, April 2026

Abstract: With the growing demand for clean and sustainable energy, efficient and eco-friendly power sources are more crucial than ever. Solar energy, though abundant and renewable, remains underutilized due to limitations in current photovoltaic technologies. Overcoming these limitations calls for innovative semiconductors that can exceed conventional efficiency limits. Defect chalcopyrite semiconductors, particularly ZnGaS have emerged as strong candidate for next-generation intermediate band solar cells (IBSCs). In this study, we employ density functional theory (DFT) to investigate the effects of transition metal (TM) substitutions (Mn, Fe, Co, and Ni) on the structural, electronic and mechanical properties of ZnGaS. Our results show that TM substitution introduces intermediate band (IB) states within the bandgap. Specifically, Co substitution exhibits well-isolated IB states, making it the most promising candidate for IBSC applications. The structural analysis indicates that TM incorporation modifies lattice parameters, with Mn causing unit cell expansion while Fe, Co, and Ni induce lattice contraction. Mechanical stability is confirmed through Born criteria and all of these TM-substituted compounds are found to be ductile in nature. Thermodynamic stability is evaluated via cohesive and formation energy calculations, where Mn-substituted ZnGaS demonstrates the strongest bonding. Additionally, melting temperature analysis indicates ZnNiGaS has the highest thermal stability (1212.387 K), whereas, ZnMnGaS has the lowest (892.856 K). These findings highlight the potential of Co-substituted ZnGaS for next-generation photovoltaic applications.

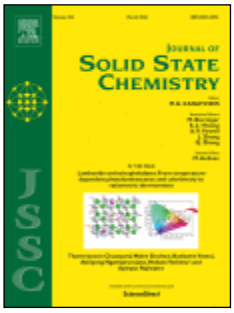

URL: https://www.sciencedirect.com/science/article/pii/S0022459625006152?

SCHOLARLY PUBLICATIONS
School of Applied Sciences
KIIT Deemed to be University

Journal Name: Inorganica Chimica Acta **IF: 3.2**

Title: Crystallographic and quantum chemical methods to elucidate the structural and electronic characteristics of a Zn(II) complex

Author: Patla, A.; Dutta, B.; Paul, A.; Subramanian, R.; Konar, S.

Details: Volume 595 , May 2026

Abstract: A new zinc(II) complex [Zn(L)$(SCN)_2$] (1) of NNN donor Schiff base ligand L (where "L" = N-(4,6-dimethyl-pyrimidin-2-yl)-N'-pyridin-2-ylmethylene-hydrazine) is synthesized and characterized by elemental analysis and single crystal X-ray crystallography (XRD). Using the single-crystal X-ray diffraction technique, the structure of Complex 1 exhibits a distorted trigonal bipyramidal geometry. The crystal packing of 1 exhibits intermolecular S···H, π···π stacking interactions to generate a 1D network. These unique S···H interactions significantly affect the stability, arrangement, and prospective functional uses of the Complex. DFT calculations were used to determine the complex's electronic structure, using the pseudo-potential LANL2DZ for the zinc atom and the 6-31G+(d,p) basis set for the remaining atoms, at the B3LYP level. At this computational level, the optimized structure can accurately replicate the crystal structure. To comprehend the complex's reactivity properties, the molecule's electrostatic potential (MEP) and frontier molecular orbital analysis have been assessed. Natural bond orbital (NBO) analysis was used to illustrate the charge transfer between donor and acceptor sites. Additionally, fingerprint plots and Hirshfeld surface analysis are used to examine the complex's intermolecular interactions. Hirshfeld surface analysis, combined with two-dimensional fingerprint plots, provided a comparative visualization of the non-covalent interaction patterns in the synthesized complex.

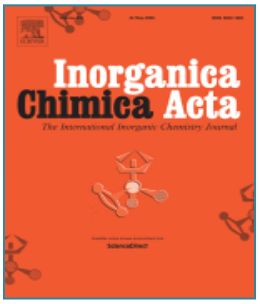

URL: https://www.sciencedirect.com/science/article/pii/S002016932600040X?via%3Dihub

Journal Name: Journal of Sol-Gel Science and Technology **IF: 3.2**

Title: Multifunctional Ce@Co3O4 nanostructures for sustainable solar-driven dye removal and microbial inhibition

Author: Pradhan, D; Biswal, SK; Pattnaik, R; Kamal, R; Nayak, N; Dash, SK

Details: Volume 117, February 2026

Abstract: The discovery and development of efficient photocatalytic materials for environmental applications is a rapidly evolving research area. This work addresses the photo degradation of RhB 6 G, a fluorescent dye, utilizing a novel heterogeneous catalyst: lanthanide metal-doped Co_3O_4. Pristine Co_3O_4 was produced using chemical sol-gel and green synthesis with Azadirachta indica leaves (Neem leaf) extract. The catalysts' structural, morphological, and optical characteristics were investigated using XRD, FT-IR, FE-SEM, HR-TEM, UV-DRS, RAMAN, BET, XPS, and PL analysis. The average diameters of the crystallites were found to be 11.47 nm (Ce-doped), 41 nm (green), and 45 nm (chemical). Based on Tauc plots, the corresponding band gap energies were 2.42 eV, 2.8 eV, and 2.9 eV, respectively. The $Ce@Co_3O_4$ catalyst's surface area increased significantly, according to the BET study (96.2 m^2/g), and PL analysis revealed lower emission intensity, which suggests suppressed charge carrier recombination. Additionally, XRD-based microstructural analysis revealed that $Ce@Co_3O_4$ exhibited the highest dislocation density and microstrain, suggesting a higher density of structural defects that may facilitate more efficient charge separation and enhanced surface reactivity. The degradation of RhB 6G under direct sunlight irradiation was used to determine photo-catalytic activity. Various parameters, such as reaction conditions, reactive species identification, mechanism, and the effects of competing species, were investigated. After 75 min of exposure to sunlight, the doped catalyst degraded by an astonishing 94%. The kinetic study confirmed that the pseudo-first order model is followed with a rate constant of 0.0541 min^{-1}. An additional dimension to its multifunctional potential was added when Ce-doped CoO_4 showed strong antibacterial activity, especially against E. coli, because of increased reactive oxygen species production. The $Ce@Co_3O_4$ composite holds great promise as a material for the degradation of diverse pollutants and antibacterial activity in future applications.

URL: https://link.springer.com/article/10.1007/s10971-025-07026-7

SCHOLARLY PUBLICATIONS
School of Applied Sciences
KIIT Deemed to be University

Journal Name: Icarus **IF: 3.0**

Title: Influence of albedo, radiation pressure, oblateness, and dust belt on the stability in the generalized elliptic restricted three-body problem

Author: Prasadu, B.R.; Mia, R.

Details: Volume 446, March 2026

Abstract: In this paper, we investigate the motion of an infinitesimal body in the framework of the modified elliptic restricted three-body problem by taking into account additional forces due to albedo, radiation pressure, the oblateness of the primaries' and the dust belt. We obtain semi-analytical solutions of locations for non-collinear equilibrium points. The positions of non-collinear equilibrium points are shown graphically for different values of perturbation parameters. To investigate the motion of the infinitesimal body, we have chosen three real astronomical systems: the Sun–Mars, Proxima Centauri, and Sun–Saturn. The effects of different perturbation parameters on the position of non-collinear equilibrium points are analysed. The linear stability analysis of equilibrium points is performed by computing the critical mass ratio. Our findings indicate that the stability and instability of non-collinear equilibrium points are influenced by the mass ratio and specific perturbation parameters associated with each system.

URL: https://www.sciencedirect.com/science/article/abs/pii/S0019103525004336?via%3Dihub